

Mono and dinuclear half-sandwich platinum group metal complexes bearing pyrazolyl-pyrimidine ligands: Syntheses and structural studies

Kota Thirumala Prasad^a, Bruno Therrien^b, Steven Geib^c, Kollipara Mohan Rao^{a,*}

^a Department of Chemistry, North Eastern Hill University, Shillong 793 022, India

^b Service Analytique Facultaire, University of Neuchâtel, Case Postale 158, CH-2009, Neuchâtel, Switzerland

^c Department of Chemistry, University of Pittsburgh, PA 15260, USA

A B S T R A C T

Reactions of 0.5 eq. of the dinuclear complexes $[(\eta^6\text{-arene})\text{Ru}(\mu\text{-Cl})\text{Cl}]_2$ (arene = $\eta^6\text{-C}_6\text{H}_6$, $\eta^6\text{-}p\text{-}^i\text{PrC}_6\text{H}_4\text{Me}$) and $[(\text{Cp}^*)\text{M}(\mu\text{-Cl})\text{Cl}]_2$ (M = Rh, Ir; $\text{Cp}^* = \eta^5\text{-C}_5\text{Me}_5$) with 4,6-disubstituted pyrazolyl-pyrimidine ligands (L) viz. 4,6-bis(pyrazolyl)pyrimidine (L1), 4,6-bis(3-methyl-pyrazolyl)pyrimidine (L2), 4,6-bis(3,5-dimethyl-pyrazolyl)pyrimidine (L3) lead to the formation of the cationic mononuclear complexes $[(\eta^6\text{-C}_6\text{H}_6)\text{Ru}(\text{L})\text{Cl}]^+$ (L = L1, **1**; L2, **2**; L3, **3**), $[(\eta^6\text{-}p\text{-}^i\text{PrC}_6\text{H}_4\text{Me})\text{Ru}(\text{L})\text{Cl}]^+$ (L = L1, **4**; L2, **5**; L3, **6**), $[(\text{Cp}^*)\text{Rh}(\text{L})\text{Cl}]^+$ (L = L1, **7**; L2, **8**; L3, **9**) and $[(\text{Cp}^*)\text{Ir}(\text{L})\text{Cl}]^+$ (L = L1, **10**; L2, **11**; L3, **12**), while reactions with 1.0 eq. of the dinuclear complexes $[(\eta^6\text{-arene})\text{Ru}(\mu\text{-Cl})\text{Cl}]_2$ and $[(\text{Cp}^*)\text{M}(\mu\text{-Cl})\text{Cl}]_2$ give rise to the dicationic dinuclear complexes $\{[(\eta^6\text{-C}_6\text{H}_6)\text{RuCl}]_2(\text{L})\}^{2+}$ (L = L1, **13**; L2, **14**; L3, **15**), $\{[(\eta^6\text{-}p\text{-}^i\text{PrC}_6\text{H}_4\text{Me})\text{RuCl}]_2(\text{L})\}^{2+}$ (L = L1, **16**; L2, **17**; L3, **18**), $\{[(\text{Cp}^*)\text{RhCl}]_2(\text{L})\}^{2+}$ (L = L1, **19**; L2, **20**; L3, **21**) and $\{[(\text{Cp}^*)\text{IrCl}]_2(\text{L})\}^{2+}$ (L = L1 **22**; L2, **23**; L3 **24**). The molecular structures of **[3]**PF₆, **[6]**PF₆, **[7]**PF₆ and **[18]**(PF₆)₂ have been established by single crystal X-ray structure analysis.

Keywords

Arene, Cp*, Pyrazolyl-pyrimidine, Ruthenium, Rhodium, Iridium

1. Introduction

During the last few decades there has been great interest in the chemistry of transition metals associated with polydentate ligands with sp²-hybridized nitrogen atoms, for instance, polypyrazolylborates [1,2] and polypyridines [2–10]. In many cases the charge transfer properties of these compounds justify this interest. Especially with these nitrogen donor ligands have been shown to be effective catalysts for oxidation reactions [11–19] and for ring-opening metathesis polymerization [20] and recent studies of arene ruthenium complexes have shown that they are found to inhibit cancer cell growth [21–26], as non-linear optical (NLO) materials [27,28]. For a majority of the complexes studied, the metal centers are linked by a bridging ligand and the nature of the bridge has a fundamental influence on the electronic interaction between the metals and therefore on the characteristics of the material.

The ligand 4,6-bis(pyrazolyl)pyrimidine (L1) and its analogues, 4,6-bis(3-methyl-pyrazolyl)pyrimidine (L2) and 4,6-bis(3,5-dimethyl-pyrazolyl)pyrimidine (L3), are the subject of this investigation. They have a structural similarity to 3,6-bis(pyrazolyl)pyridazine (**A**) and 4,5-bis(pyrazolyl)quinoxaline (**B**) both of which have been previously studied [29,30]. In our previous work, we demonstrated that the ligand **A** does not yield dinuclear compounds with two half-sandwich platinum group metal atoms, since

the steric nature of the ligand, resulted only in the formation of mononuclear complexes [29]. However it is true in the case of more sterically free ligand **B** also, because it also yielded mononuclear complexes, since the pyrazole rings of the ligand tilted with respect to the central quinoxaline ring because of the steric collide between the R' groups of the pyrazole rings. In the case of ligand **A** the pyrazolyl rings are bonded *para* to each other, where as in the case of ligand **B**, they are bonded *ortho* to each other on central six membered rings. But sterically less demanding ligand L (L1–L3) can coordinate to two half-sandwich platinum group metal centers, since the pyrazolyl rings of the ligand are bonded *meta* to each other, leading to reduced steric interaction, which enhances the stability of the dinuclear complexes.

In recent years, we have been carrying out arene ruthenium complexation reactions with a variety of nitrogen-based ligands [31–36] including pyridyl-pyridazine and pyrazolyl-pyridazine ligands. Ruthenium complexes of these types of nitrogen-based ligands have a capacity to function as catalysts for the oxidation of water to oxygen [37–39]. Although extensive studies have been made on ruthenium complexes containing polypyridyl ligands, complexes containing pyrazolyl-pyrimidine ligands have not yet been investigated.

In the present paper, we focus on the synthetic methodology applied for the development of homogeneous and immobilized half-sandwich ruthenium, rhodium and iridium complexes bearing bis(pyrazolyl)pyrimidine, as a specific *N,N*-bidentate bridging ligands (L) (Scheme 1).

* Corresponding author. Tel.: +91 364 272 2620; fax: +91 364 272 1010.

E-mail address: mohanrao59@gmail.com (K.M. Rao).

Table 1Details of the data collection and results of the structure refinement parameters for complexes [3]PF₆·H₂O, [6]PF₆, [7]PF₆ and [18](PF₆)₂·H₂O.

Complex	[3]PF ₆ ·H ₂ O	[6]PF ₆	[7]PF ₆	[18](PF ₆) ₂ ·H ₂ O
Chemical formula	C ₂₀ H ₂₂ ClF ₆ N ₆ OPRu	C ₂₄ H ₃₀ ClF ₆ N ₆ PRu	C ₂₀ H ₂₃ ClF ₆ N ₆ PRh	C ₃₄ H ₄₆ Cl ₂ F ₁₂ N ₆ OP ₂ Ru ₂
Formula weight	628.03	684.03	630.77	1117.75
Crystal system	Triclinic	Triclinic	Triclinic	Monoclinic
Space group	<i>P</i> $\bar{1}$	<i>P</i> $\bar{1}$	<i>P</i> $\bar{1}$	<i>P</i> 2 ₁ / <i>a</i>
Crystal color and shape	Orange blade	Red block	Red block	Orange block
Crystal size (mm)	0.25 × 0.12 × 0.12	0.28 × 0.28 × 0.18	0.50 × 0.26 × 0.15	0.21 × 0.18 × 0.13
<i>a</i> (Å)	8.4350(11)	8.4928(10)	7.5841(6)	17.1745(13)
<i>b</i> (Å)	9.1359(12)	12.1384(14)	11.2581(10)	13.5980(8)
<i>c</i> (Å)	16.328(2)	14.1361(16)	14.7304(12)	17.6465(11)
α (°)	91.340(2)	99.418(2)	74.056(2)	90.00
β (°)	92.071(2)	90.677(2)	88.015(2)	90.062(8)
γ (°)	105.129(2)	104.611(2)	88.408(2)	90.00
<i>V</i> (Å ³)	1213.2(3)	1389.0(3)	1208.39(17)	4121.1(5)
<i>Z</i>	2	2	2	4
<i>T</i> (K)	203(2)	203(2)	203(2)	173(2)
<i>D_x</i> (g/cm ³)	1.763	1.636	1.734	1.802
μ (mm ⁻¹)	0.895	0.785	0.952	1.033
Scan range (°)	2.31 < θ < 28.31	1.76 < θ < 32.38	1.88 < θ < 32.33	1.91 < θ < 26.08
Unique reflections	12 483	17 438	14 825	8096
Reflections used [<i>I</i> > 2 σ (<i>I</i>)]	5998	9027	7813	5203
<i>R</i> _{int}	0.0260	0.0383	0.0244	0.0644
Final <i>R</i> indices [<i>I</i> > 2 σ (<i>I</i>)]	0.0385, <i>wR</i> ₂ 0.1160	0.0513, <i>wR</i> ₂ 0.1368	0.0428, <i>wR</i> ₂ = 0.1387	0.0379, <i>wR</i> ₂ = 0.0791
<i>R</i> indices (all data)	0.0415, <i>wR</i> ₂ 0.1203	0.0615, <i>wR</i> ₂ 0.1471	0.0463, <i>wR</i> ₂ = 0.1437	0.0700, <i>wR</i> ₂ = 0.0862
Goodness-of-fit (GOF)	1.186	1.121	1.178	0.849
Maximum, Minimum $\Delta\rho$ (e Å ⁻³)	1.183, -0.564	1.128, -0.754	1.214, -1.051	0.949, -0.807

Table 2Selected bond lengths and angles for complexes [3]PF₆·H₂O, [6]PF₆, [7]PF₆ and [18](PF₆)₂·H₂O.

	[3]PF ₆	[6]PF ₆	[7]PF ₆	[18](PF ₆) ₂
<i>Distances</i> (Å)				
M1–Cl1	2.402(7)	2.388(8)	2.40(6)	2.393(1)
M2–Cl2	–	–	–	2.391(1)
M1–N1	2.076(2)	2.102(2)	2.106(2)	2.072(3)
M1–N3	2.092(2)	2.093(2)	2.138(2)	2.092(3)
M2–N4	–	–	–	2.092(3)
M2–N6	–	–	–	2.076(3)
M1–centroid ^a	1.690	1.685	1.770	1.685
M2–centroid ^a	–	–	–	1.678
<i>Angles</i> (°)				
N1–M1–N3	75.33(7)	75.56(9)	75.34(8)	75.70(1)
N4–M2–N6	–	–	–	75.0(1)
N1–M1–Cl1	84.76(6)	87.51(7)	90.43(7)	82.86(3)
N4–M2–Cl2	–	–	–	84.26(9)
N3–M1–Cl1	84.09(6)	84.27(7)	84.73(6)	83.31(9)
N6–M2–Cl2	–	–	–	81.70(9)

^a Calculated centroid-to-metal distances (η^6 -C₆ or η^5 -C₅ coordinated aromatic ring).

³*J* = 2.4 Hz), 8.66 (d, 1H, ³*J* = 7.6 Hz), 8.63 (d, 1H, ³*J* = 7.6 Hz), 8.29 (s, 1H), 8.02 (s, 1H), 6.96 (dd, 1H, ³*J* = 2.0 Hz), 6.67 (dd, 1H, ³*J* = 1.6 Hz), 6.07 (s, 6H, C₆H₆); ESI-MS (*m/z*): 427.2 [M–PF₆]⁺, 392.1 [M–PF₆–Cl]⁺, 314.1 [M–PF₆–Cl–C₆H₆]⁺; IR (KBr, cm⁻¹): 844s $\nu_{(P-F)}$, 1522m, 1558m, 1608s ($\nu_{C=N}$ L1), 2925m, 3446w; UV–Vis {acetonitrile, λ_{max} nm (ϵ 10⁻⁵M⁻¹ cm⁻¹): 246(0.16), 324(0.17), 381(0.25), 464(0.04).

2.4.2. [(η^6 -C₆H₆)Ru(L2)Cl]PF₆ ([2]PF₆)

Yield: 62 mg, 74.6%.

Elemental Anal. Calc. for C₁₈H₁₈N₆RuClPF₆ (599.86): C, 39.91; H, 3.35; N, 15.51. Found: C, 40.22; H, 3.08; N, 14.92%. ¹H NMR (400 MHz, CD₃CN, 25 °C, TMS): δ = 9.15 (s, 1H), 8.54 (d, 1H, ³*J* = 8.4 Hz), 8.09 (s, 1H), 7.50 (d, 1H, ³*J* = 4.6 Hz), 7.21 (d, 1H, ³*J* = 4.6 Hz), 6.92 (d, 1H, ³*J* = 2.8 Hz), 6.24 (s, 6H, C₆H₆), 2.83 (s, 3H, CH₃), 2.76 (s, 3H, CH₃); ESI-MS (*m/z*): 455.2 [M–PF₆]⁺, 419.2 [M–PF₆–Cl]⁺, 341.1 [M–PF₆–Cl–C₆H₆]⁺; IR (KBr, cm⁻¹): 845s $\nu_{(P-F)}$, 1592m, 1558m, 1522m ($\nu_{C=N}$ L2), 2925m, 3434w; UV–Vis {acetonitrile, λ_{max} nm (ϵ 10⁻⁵M⁻¹ cm⁻¹): 319(0.23), 345(0.18), 456(0.04).

2.4.3. [(η^6 -C₆H₆)Ru(L3)Cl]PF₆ ([3]PF₆)

Yield: 65 mg, 86.3%.

Elemental Anal. Calc. for C₂₀H₂₂N₆RuClPF₆ (628.03): C, 42.16; H, 3.89; N, 14.75. Found: C, 41.90; H, 4.05; N, 14.33%. ¹H NMR (400 MHz, CD₃CN): δ = 9.44 (s, 1H), 8.17 (s, 1H), 7.39 (s, 1H), 6.53 (s, 1H), 6.10 (s, 6H, C₆H₆), 2.82 (s, 3H, CH₃), 2.76 (s, 3H, CH₃), 2.75 (s, 3H, CH₃), 2.29 (s, 3H, CH₃); ESI-MS (*m/z*): 483.3 [M–PF₆]⁺, 448.2 [M–PF₆–Cl]⁺, 413.3 [M–PF₆–Cl–C₆H₆]⁺; IR (KBr, cm⁻¹): 845s $\nu_{(P-F)}$, 1601m, 1560m, 1525m ($\nu_{C=N}$ L3), 2925m, 3482w; UV–Vis {acetonitrile, λ_{max} nm (ϵ 10⁻⁵M⁻¹ cm⁻¹): 273(0.15), 309(0.15), 354(0.25), 452(0.06).

2.4.4. [(η^6 -*p*-ⁱPrC₆H₄Me)Ru(L1)Cl]PF₆ ([4]PF₆)

Yield: 65 mg, 75.5%.

Elemental Anal. Calc. for C₂₀H₂₂N₆RuClPF₆ (628.03): C, 38.26; H, 3.53; N, 13.38. Found: C, 37.92; H, 3.77; N, 12.95%. ¹H NMR (400 MHz, CDCl₃): δ = 9.48 (d, 1H, ³*J* = 2.4 Hz), 8.77 (d, 1H, ³*J* = 2.4 Hz, 1H), 8.67 (d, 1H, ³*J* = 4.6 Hz), 8.61 (d, 1H, ³*J* = 6.4 Hz), 8.29 (s, 1H), 7.97 (s, 1H), 6.96 (dd, 1H, ³*J* = 2.0 Hz), 6.69 (dd, 1H, ³*J* = 2.0 Hz), 6.04 (d, 1H, ³*J*_{H,H} = 6.4 Hz, Ar_{p-cy}), 6.07 (d, 1H, ³*J* = 6.4 Hz, Ar_{p-cy}), 5.99 (d, 1H, ³*J* = 6.0 Hz, Ar_{p-cy}), 5.86 (d, 1H, ³*J* = 6.0 Hz, Ar_{p-cy}), 2.74 (sept, 1H, ³*J* = 6.2 Hz, CH(CH₃)₂), 2.18 (s, 3H, Ar_{p-cy}-Me), 1.14 (d, 3H, ³*J* = 6.4 Hz, CH(CH₃)₂), 1.10 (d, 3H, ³*J* = 7.6 Hz, CH(CH₃)₂); ESI-MS (*m/z*): 483.1 [M–PF₆]⁺, 448.1 [M–PF₆–Cl]⁺, 314.1 [M–PF₆–Cl-*p*-ⁱPrC₆H₄Me]⁺; IR (KBr, cm⁻¹): 844s $\nu_{(P-F)}$, 1605m, 1557m, 1523m ($\nu_{C=N}$ L1), 3058m, 3489w; UV–Vis {acetonitrile, λ_{max} nm (ϵ 10⁻⁵M⁻¹ cm⁻¹): 286(0.65), 333(0.21), 436(0.02).

2.4.5. [(η^6 -*p*-ⁱPrC₆H₄Me)Ru(L2)Cl]PF₆ ([5]PF₆)

Yield: 68 mg, 73.4%.

Elemental Anal. Calc. for C₂₂H₂₆N₆RuClPF₆ (651.06): C, 43.28; H, 4.29; N, 13.77. Found: C, 43.78; H, 3.94; N, 13.92%. ¹H NMR (400 MHz, CDCl₃): δ = 9.25 (s, 1H), 8.48 (d, 1H, ³*J* = 2.4 Hz), 7.89 (s, 1H), 7.78 (d, 1H, ³*J* = 2.8 Hz), 6.70 (d, 1H, ³*J* = 9.6 Hz), 6.39 (d, 1H, ³*J* = 2.8 Hz), 5.98 (d, 2H, ³*J* = 6.0 Hz, Ar_{p-cy}), 5.90 (d, 1H, ³*J* = 6.0 Hz, Ar_{p-cy}), 5.86 (d, 1H, ³*J* = 6.0 Hz, Ar_{p-cy}), 2.81 (s, 3H, CH₃), 2.75 (sept, 1H, CH(CH₃)₂), 2.38 (s, 3H, CH₃), 2.18 (s, 3H, Ar_{p-cy}-Me), 1.42 (d, 3H, ³*J* = 3.2 Hz, CH(CH₃)₂), 1.17 (d, 3H, ³*J* = 3.2 Hz,

CH(CH₃)₂); ESI-MS (*m/z*): 513.2 [M–PF₆]⁺, 478.6 [M–PF₆-Cl]⁺, 344.2 [M–PF₆-Cl-*p*-ⁱPrC₆H₄Me]⁺; IR (KBr, cm⁻¹): 843s $\nu_{(P-F)}$, 1606m, 1560m, 1524m ($\nu_{C=N}$ L2), 2995m, 3447w; UV-Vis {acetonitrile, λ_{max} nm ($\epsilon 10^{-5} M^{-1} cm^{-1}$): 294(0.36), 349(0.82), 470(0.02).

2.4.6. [(η^6 -*p*-ⁱPrC₆H₄Me)Ru(L3)Cl]PF₆ (**[6]**PF₆)

Yield: 77 mg, 82.7%.

Elemental Anal. Calc. for C₂₄H₃₀N₆RuClPF₆ (684.09): C, 46.06; H, 4.83; N, 13.43. Found: C, 46.73; H, 4.25; N, 13.07%. ¹H NMR (400 MHz, CDCl₃): δ = 9.44 (s, 1H), 8.11 (s, 1H), 7.32 (s, 1H), 7.05 (s, 1H), 5.96 (d, 1H, ³J = 4.0 Hz, Ar_{*p*-cy}), 5.92 (d, 1H, ³J = 3.2 Hz, Ar_{*p*-cy}), 5.84 (d, 1H, ³J = 6.4 Hz, Ar_{*p*-cy}), 5.77 (d, 1H, ³J = 6.4 Hz, Ar_{*p*-cy}), 2.81 (s, 3H, CH₃), 2.79 (s, 3H, CH₃), 2.81 (s, 3H, CH₃), 2.78 (s, 3H, CH₃), 2.49 (sept, 1H, CH(CH₃)₂), 2.17 (s, 3H, Ar_{*p*-cy}-Me), 1.09 (d, 3H, ³J = 3.2 Hz, CH(CH₃)₂), 1.06 (d, 3H, ³J = 3.2 Hz, CH(CH₃)₂); ESI-MS (*m/z*): 538.8 [M–PF₆]⁺, 503.5 [M–PF₆-Cl]⁺, 369.2 [M–PF₆-Cl-*p*-ⁱPrC₆H₄Me]⁺; IR (KBr, cm⁻¹): 843s $\nu_{(P-F)}$, 1608m, 1560m, 1527m ($\nu_{C=N}$ L3), 3050m, 3447w; UV-Vis {acetonitrile, λ_{max} nm ($\epsilon 10^{-5} M^{-1} cm^{-1}$): 287(0.38), 346(0.74), 477(0.08).

2.5. General procedure for the preparation of the mononuclear complexes 7–12

A mixture of [(η^5 -C₅Me₅)M(μ -Cl)Cl]₂ (M = Rh and Ir) (0.08 mmol), ligand L (L1, L2 and L3) (0.17 mmol) and 2.5 equivalents of NH₄PF₆ in dry methanol (20 ml) was refluxed at 50 °C temperature for 4–6 h, resulting yellow color precipitation. The precipitate was separated by filtration, washed with cold methanol, diethyl ether and dried *in vacuo*.

2.5.1. [(Cp*)Rh(L1)Cl]PF₆ (**[7]**PF₆)

Yield: 73 mg, 77.8%.

Elemental Anal. Calc. for C₂₀H₂₃N₆RhClPF₆ (630.04): C, 38.08; H, 3.68; N, 13.98. Found: C, 38.13; H, 3.75; N, 13.91%. ¹H NMR (400 MHz, CD₃CN): δ = 9.01 (s, 1H), 8.84 (d, 1H, ³J = 3.2 Hz), 8.66 (d, 1H, ³J = 2.4 Hz), 8.33 (d, 1H, ³J = 1.6 Hz), 8.31 (d, 1H, ³J = 1.6 Hz), 7.98 (s, 1H), 7.02 (dd, 1H, ³J = 1.6 Hz), 6.71 (dd, 1H, ³J = 1.6 Hz), 1.75 (s, 15H, C₅Me₅); ESI-MS (*m/z*): 485.2 [M–PF₆]⁺, 450.6 [M–PF₆-Cl]⁺, 315.2 [M–PF₆-Cl-Cp*]⁺; IR (KBr, cm⁻¹): 844s $\nu_{(P-F)}$, 1606m, 1560m, 1524m ($\nu_{C=N}$ L1), 2999m, 3448w; UV-Vis {acetonitrile, λ_{max} nm ($\epsilon 10^{-5} M^{-1} cm^{-1}$): 268(0.78), 286(0.76), 357(0.4), 444(0.09).

2.5.2. [(Cp*)Rh(L2)Cl]PF₆ (**[8]**PF₆)

Yield: 65 mg, 62.5%.

Elemental Anal. Calc. for C₂₂H₂₇N₆RhClPF₆ (658.07): C, 35.32; H, 3.64; N, 11.23. Found: C, 35.26; H, 3.69; N, 11.21%. ¹H NMR (400 MHz, CD₃CN): δ = 8.78 (s, 1H), 8.43 (d, 1H, ³J = 6.4 Hz), 8.09 (s, 1H), 6.76 (d, 1H, ³J = 4.6 Hz), 6.40 (d, 1H, ³J = 4.6 Hz), 6.32 (d, 1H, ³J = 2.8 Hz), 2.70 (s, 3H, CH₃), 2.43 (s, 3H, CH₃), 1.77 (s, 15H, C₅Me₅); ESI-MS (*m/z*): 513.8 [M–PF₆]⁺, 478.12 [M–PF₆-Cl]⁺, 343.2 [M–PF₆-Cl-Cp*]⁺; IR (KBr, cm⁻¹): 845s $\nu_{(P-F)}$, 1598m, 1559m, 1521m ($\nu_{C=N}$ L2), 2995m, 3447w; UV-Vis {acetonitrile, λ_{max} nm ($\epsilon 10^{-5} M^{-1} cm^{-1}$): 266(0.54), 301(0.45), 343(0.57), 452(0.07).

2.5.3. [(Cp*)Rh(L3)Cl]PF₆ (**[9]**PF₆)

Yield: 78 mg, 72%.

Elemental Anal. Calc. for C₂₄H₃₁N₆RhClPF₆ (686.87): C, 41.97; H, 4.55; N, 12.24. Found: C, 41.86; H, 4.65; N, 12.18%. ¹H NMR (400 MHz, CD₃CN): δ = 9.05 (s, 1H), 8.67 (s, 1H), 7.40 (s, 1H), 6.66 (s, 1H), 2.82 (s, 3H, CH₃), 2.76 (s, 3H, CH₃), 2.75 (s, 3H, CH₃), 2.29 (s, 3H, CH₃), 2.01 (s, 15H, C₅Me₅); ESI-MS (*m/z*): 541.81 [M–PF₆]⁺, 506.6 [M–PF₆-Cl]⁺, 371.2 [M–PF₆-Cl-Cp*]⁺; IR (KBr, cm⁻¹): 843s $\nu_{(P-F)}$, 1601m, 1557m, 1524m ($\nu_{C=N}$ L3), 3050m, 3434w; UV-Vis {acetonitrile, λ_{max} nm ($\epsilon 10^{-5} M^{-1} cm^{-1}$): 261(0.09), 314(0.61), 441(0.05).

2.5.4. [(Cp*)Ir(L1)Cl]PF₆ (**[10]**PF₆)

Yield: 66 mg, 58.4%.

Elemental Anal. Calc. for C₂₀H₂₃N₆IrClPF₆ (720.09): C, 33.61; H, 2.47; N, 14.70. Found: C, 33.73; H, 2.65; N, 13.98%. ¹H NMR (400 MHz, CD₃CN): δ = 8.99 (s, 1H), 8.84 (d, 1H, ³J = 3.2 Hz), 8.66 (d, 1H, ³J = 2.4 Hz), 8.39 (d, 1H, ³J_{H,H} = 1.6 Hz), 8.32 (d, 1H, ³J_{H,H} = 1.6 Hz), 7.98 (s, 1H), 7.01 (dd, 1H, ³J_{H,H} = 1.6 Hz), 6.70 (dd, 1H, ³J_{H,H} = 2.0 Hz), 2.01 (s, 15H, C₅Me₅); ESI-MS (*m/z*): 575.2 [M–PF₆]⁺, 535.6 [M–PF₆-Cl]⁺, 400.2 [M–PF₆-Cl-Cp*]⁺; IR (KBr, cm⁻¹): 845s $\nu_{(P-F)}$, 1592m, 1558m, 1522m ($\nu_{C=N}$ L1), 2924m, 3439w; UV-Vis {acetonitrile, λ_{max} nm ($\epsilon 10^{-5} M^{-1} cm^{-1}$): 279(0.53), 340(0.89), 402(0.20).

2.5.5. [(Cp*)Ir(L2)Cl]PF₆ (**[11]**PF₆)

Yield: 70 mg, 57.8%.

Elemental Anal. Calc. for C₂₂H₂₇N₆IrClPF₆ (748.13): C, 35.32; H, 3.64; N, 11.23. Found: C, 35.25; H, 3.68; N, 11.22%. ¹H NMR (400 MHz, CD₃CN): δ = 8.78 (s, 1H), 8.43 (d, 1H, ³J = 6.4 Hz), 8.09 (s, 1H), 6.76 (d, 1H, ³J = 4.6 Hz), 6.40 (d, 1H, ³J = 4.6 Hz), 6.32 (d, 1H, ³J = 2.8 Hz), 2.70 (s, 3H, CH₃), 2.43 (s, 3H, CH₃), 1.77 (s, 15H, C₅Me₅); ESI-MS (*m/z*): 603.1 [M–PF₆]⁺, 568.2 [M–PF₆-Cl]⁺, 433.2 [M–PF₆-Cl-Cp*]⁺; IR (KBr, cm⁻¹): 845s $\nu_{(P-F)}$, 1598m, 1559m, 1521m ($\nu_{C=N}$ L2), 2995m, 3446w; UV-Vis {acetonitrile, λ_{max} nm ($\epsilon 10^{-5} M^{-1} cm^{-1}$): 267(0.54), 298(0.82), 429(0.08).

2.5.6. [(Cp*)Ir(L3)Cl]PF₆ (**[12]**PF₆)

Yield: 78 mg, 64.4%.

Elemental Anal. Calc. for C₂₄H₃₁N₆IrClPF₆ (776.96): C, 37.14; H, 4.03; N, 10.83. Found: C, 37.06; H, 4.05; N, 10.33%. ¹H NMR (400 MHz, CD₃CN): δ = 8.90 (s, 1H), 8.21 (s, 1H), 6.67 (s, 1H), 6.20 (s, 1H), 2.83 (s, 3H, CH₃), 2.76 (s, 3H, CH₃), 2.64 (s, 3H, CH₃), 2.30 (s, 3H, CH₃), 2.15 (s, 15H, C₅Me₅); ESI-MS (*m/z*): 631.2 [M–PF₆]⁺, 596.6 [M–PF₆-Cl]⁺, 461.2 [M–PF₆-Cl-Cp*]⁺; IR (KBr, cm⁻¹): 843s $\nu_{(P-F)}$, 1606m, 1560m, 1524m ($\nu_{C=N}$ L2), 3050m, 3446w; UV-Vis {acetonitrile, λ_{max} nm ($\epsilon 10^{-5} M^{-1} cm^{-1}$): 268(0.50), 301(0.41), 361(0.51) and 464(0.04).

2.6. General procedure for the preparation of the dinuclear complexes 13–18

A mixture of [(η^6 -arene)Ru(μ -Cl)Cl]₂ (arene = C₆H₆ and η^6 -*p*-ⁱPrC₆H₄Me) (0.1 mmol), ligand L (L1, L2 and L3) (0.1 mmol) and 2.5 equivalents of NH₄PF₆ in dry methanol (15 ml) was stirred at room temperature for 14 h resulting orange color precipitation. The precipitate was filtered, washed with cold methanol, diethyl ether and dried *in vacuo*.

2.6.1. {[(η^6 -C₆H₆)RuCl]₂(L1)}(PF₆)₂ (**[13]**(PF₆)₂)

Yield: 72 mg, 77.4%.

Elemental Anal. Calc. for C₂₂H₂₀N₆Ru₂Cl₂P₂F₁₂ (931.41): C, 28.37; H, 2.16; N, 9.02. Found: C, 28.21; H, 2.45; N, 8.98%. ¹H NMR (400 MHz, CD₃CN): δ = 9.68 (d, 2H, ³J = 2.8 Hz), 8.79 (s, 1H), 8.71 (d, 2H, ³J = 7.2 Hz), 8.32 (s, 1H), 7.01 (dd, 2H, ³J = 2.0 Hz), 6.15 (s, 12H, C₆H₆); ESI-MS (*m/z*): 786.1 [M²⁺+PF₆]⁺, 427.2 [M–PF₆]⁺; IR (KBr, cm⁻¹): 845s $\nu_{(P-F)}$, 1598m, 1559m, 1521m ($\nu_{C=N}$ L1), 2995m, 3447w; UV-Vis {acetonitrile, λ_{max} nm ($\epsilon 10^{-5} M^{-1} cm^{-1}$): 259(0.21), 318(0.23), 380(0.08).

2.6.2. {[(η^6 -C₆H₆)RuCl]₂(L2)}(PF₆)₂ (**[14]**(PF₆)₂)

Yield: 71 mg, 74.7%.

Elemental Anal. Calc. for C₂₄H₂₄N₆Ru₂Cl₂P₂F₁₂ (959.46): C, 30.04; H, 2.52; N, 8.76. Found: C, 29.95; H, 2.58; N, 8.61%. ¹H NMR (400 MHz, CD₃CN): δ = 9.46 (s, 1H), 8.58 (d, 2H, ³J = 8.4 Hz), 8.15 (s, 1H), 7.25 (d, 2H, ³J = 4.6 Hz), 6.24 (s, 12H, C₆H₆), 2.83 (s, 3H, CH₃), 2.81 (s, 3H, CH₃); ESI-MS (*m/z*): 814.2 [M²⁺+PF₆]⁺, 455.2 [M–PF₆]⁺; IR (KBr, cm⁻¹): 843s $\nu_{(P-F)}$, 1601m, 1557m, 1524m ($\nu_{C=N}$

L2), 3010m, 3449w; UV-Vis {acetonitrile, λ_{\max} nm ($\epsilon 10^{-5} \text{M}^{-1} \text{cm}^{-1}$): 262(0.29), 310(0.75), 374(0.12).

2.6.3. $\{[(\eta^6\text{-C}_6\text{H}_6)\text{RuCl}_2(\text{L3})](\text{PF}_6)_2\}$ (**[15]**(PF_6)₂)

Yield: 81 mg, 82.6%.

Elemental Anal. Calc. for $\text{C}_{24}\text{H}_{28}\text{N}_6\text{Ru}_2\text{Cl}_2\text{P}_2\text{F}_{12}$ (987.52): C, 31.62; H, 2.86; N, 8.51. Found: C, 31.50; H, 2.95; N, 8.33%. ^1H NMR (400 MHz, CD_3CN): $\delta = 10.02$ (s, 1H), 7.68 (s, 1H), 6.72 (s, 2H), 6.21 (s, 12H, C_6H_6), 2.81 (s, 6H, CH_3), 2.69 (s, 6H, CH_3); ESI-MS (m/z): 842.4 $[\text{M}^{2+} + \text{PF}_6^-]^+$, 483.3 $[\text{M} - \text{PF}_6]^+$; IR (KBr, cm^{-1}): 843s $\nu_{(\text{P-F})}$, 1606m, 1560m, 1524m ($\nu_{\text{C=N}}$ L3), 3050m, 3451w; UV-Vis {acetonitrile, λ_{\max} nm ($\epsilon 10^{-5} \text{M}^{-1} \text{cm}^{-1}$): 271(0.18), 315(0.81), 380(0.11).

2.6.4. $\{[(\eta^6\text{-p-}^i\text{PrC}_6\text{H}_4\text{Me})\text{RuCl}_2(\text{L1})](\text{PF}_6)_2\}$ (**[16]**(PF_6)₂)

Yield: 87 mg, 83.6%.

Elemental Anal. Calc. for $\text{C}_{30}\text{H}_{38}\text{N}_6\text{Ru}_2\text{Cl}_2\text{P}_2\text{F}_{12}$ (1043.62): C, 34.53; H, 3.48; N, 8.05. Found: C, 34.42; H, 3.47; N, 7.96%. ^1H NMR (400 MHz, CDCl_3): $\delta = 9.65$ (d, 2H, $^3J = 2.4$ Hz), 8.71 (d, 2H, $^3J = 4.6$ Hz), 8.68 (s, 1H), 7.28 (s, 1H), 7.06 (dd, 2H, $^3J = 2.4$ Hz), 6.08 (d, 2H, $^3J = 6.4$ Hz, $\text{Ar}_{\text{p-cy}}$), 6.06 (d, 2H, $^3J = 6.4$ Hz, $\text{Ar}_{\text{p-cy}}$), 5.99 (d, 2H, $^3J = 6.0$ Hz, $\text{Ar}_{\text{p-cy}}$), 5.93 (d, 2H, $^3J = 6.0$ Hz, $\text{Ar}_{\text{p-cy}}$), 2.74–2.69 (sept, 2H, $^3J = 6.2$ Hz, $\text{CH}(\text{CH}_3)_2$), 2.18 (s, 6H, $\text{Ar}_{\text{p-cy}}\text{-Me}$), 1.14 (d, 6H, $^3J = 6.8$ Hz, $\text{CH}(\text{CH}_3)_2$), 1.04 (d, 6H, $^3J = 7.6$ Hz, $\text{CH}(\text{CH}_3)_2$); ESI-MS (m/z): 898.2 $[\text{M}^{2+} + \text{PF}_6^-]^+$, 483.3 $[\text{M} - \text{PF}_6]^+$; IR (KBr, cm^{-1}): 844s $\nu_{(\text{P-F})}$, 1599m, 1560m, 1525m ($\nu_{\text{C=N}}$ L1), 2995m, 3447w; UV-Vis {acetonitrile, λ_{\max} nm ($\epsilon 10^{-5} \text{M}^{-1} \text{cm}^{-1}$): 260(0.29), 310(0.58), 378(0.13).

2.6.5. $\{[(\eta^6\text{-p-}^i\text{PrC}_6\text{H}_4\text{Me})\text{RuCl}_2(\text{L2})](\text{PF}_6)_2\}$ (**[17]**(PF_6)₂)

Yield: 77 mg, 71.9%.

Elemental Anal. Calc. for $\text{C}_{32}\text{H}_{40}\text{N}_6\text{Ru}_2\text{Cl}_2\text{P}_2\text{F}_{12}$ (1071.67): C, 35.86; H, 3.76; N, 7.84. Found: C, 43.78; H, 3.94; N, 13.92%. ^1H NMR (400 MHz, CDCl_3): $\delta = 9.38$ (s, 1H), 8.51 (d, 2H, $^3J = 2.8$ Hz), 7.89 (s, 1H), 6.75 (d, 2H, $^3J = 9.6$ Hz), 6.01 (d, 2H, $^3J = 6.0$ Hz, $\text{Ar}_{\text{p-cy}}$), 5.99 (d, 2H, $^3J = 6.04$ Hz, $\text{Ar}_{\text{p-cy}}$), 5.96 (d, 2H, $^3J = 6.0$ Hz, $\text{Ar}_{\text{p-cy}}$), 5.96 (d, 2H, $^3J = 6.04$ Hz, $\text{Ar}_{\text{p-cy}}$), 2.81 (s, 6H, CH_3), 2.75 (sept, 2H, $\text{CH}(\text{CH}_3)_2$), 2.26 (s, 6H, $\text{Ar}_{\text{p-cy}}\text{-Me}$), 1.19 (d, 6H, $^3J = 3.2$ Hz, $\text{CH}(\text{CH}_3)_2$), 1.17 (d, 6H, $^3J = 3.2$ Hz, $\text{CH}(\text{CH}_3)_2$); ESI-MS (m/z): 926.2 $[\text{M}^{2+} + \text{PF}_6^-]^+$, 513.2 $[\text{M} - \text{PF}_6]^+$; IR (KBr, cm^{-1}): 843s $\nu_{(\text{P-F})}$, 1601m, 1557m, 1524m ($\nu_{\text{C=N}}$ L2), 3011m, 3451w; UV-Vis {acetonitrile, λ_{\max} nm ($\epsilon 10^{-5} \text{M}^{-1} \text{cm}^{-1}$): 271(0.18), 315(0.81), 380(0.11).

2.6.6. $\{[(\eta^6\text{-p-}^i\text{PrC}_6\text{H}_4\text{Me})\text{RuCl}_2(\text{L3})](\text{PF}_6)_2\}$ (**[18]**(PF_6)₂)

Yield: 90 mg, 82.5%.

Elemental Anal. Calc. for $\text{C}_{34}\text{H}_{44}\text{N}_6\text{Ru}_2\text{Cl}_2\text{P}_2\text{F}_{12}$ (1099.73): C, 37.13; H, 4.03; N, 7.64. Found: C, 37.05; H, 4.07; N, 7.64. ^1H NMR (400 MHz, CDCl_3): $\delta = 9.91$ (s, 1H), 7.67 (s, 1H), 6.68 (s, 2H), 6.11 (d, 2H, $^3J = 6.4$ Hz, $\text{Ar}_{\text{p-cy}}$), 6.08 (d, 2H, $^3J = 6.2$ Hz, $\text{Ar}_{\text{p-cy}}$), 5.95 (d, 2H, $^3J = 6.0$ Hz, $\text{Ar}_{\text{p-cy}}$), 5.89 (d, 2H, $^3J = 6.4$ Hz, $\text{Ar}_{\text{p-cy}}$), 2.80 (s, 6H, CH_3), 2.76 (s, 6H, CH_3), 2.66 (sept, 2H, $\text{CH}(\text{CH}_3)_2$), 2.28 (s, 6H, $\text{Ar}_{\text{p-cy}}\text{-Me}$), 1.09 (d, 6H, $^3J = 3.2$ Hz, $\text{CH}(\text{CH}_3)_2$), 1.06 (d, 6H, $^3J = 3.2$ Hz, $\text{CH}(\text{CH}_3)_2$); ESI-MS (m/z): 954.73 $[\text{M}^{2+} + \text{PF}_6^-]^+$, 538.8 $[\text{M} - \text{PF}_6]^+$; IR (KBr, cm^{-1}): 843s $\nu_{(\text{P-F})}$, 1608m, 1562m, 1524m ($\nu_{\text{C=N}}$ L3), 3041m, 3447w; UV-Vis {acetonitrile, λ_{\max} nm ($\epsilon 10^{-5} \text{M}^{-1} \text{cm}^{-1}$): 263(0.29), 310(0.75), 376(0.12).

2.7. General procedure for the preparation of the dinuclear complexes **19–24**

A mixture of $[(\text{Cp}^*)\text{M}(\mu\text{-Cl})\text{Cl}]_2$ (M = Rh and Ir) (0.08 mmol), ligand L (L1, L2 and L3) (0.08 mmol) and 2.5 equivalents of NH_4PF_6 in dry methanol (20 ml) was refluxed at 50 °C for 12 h, resulting a orange color precipitation. The precipitate was separated by filtration, washed with cold methanol, diethyl ether and dried *in vacuo*.

2.7.1. $\{[(\text{Cp}^*)\text{RhCl}_2(\text{L1})](\text{PF}_6)_2\}$ (**[19]**(PF_6)₂)

Yield: 66 mg, 79.5%.

Elemental Anal. Calc. for $\text{C}_{30}\text{H}_{38}\text{N}_6\text{Rh}_2\text{Cl}_2\text{P}_2\text{F}_{12}$ (1049.31): C, 34.34; H, 3.65; N, 8.01. Found: C, 34.23; H, 3.75; N, 7.91%. ^1H NMR (400 MHz, CD_3CN): $\delta = 9.18$ (s, 1H), 8.84 (d, 2H, $^3J = 3.2$ Hz), 8.36 (d, 2H, $^3J = 1.6$ Hz), 8.01 (s, 1H), 6.92 (dd, 2H, $^3J = 1.6$ Hz), 1.81 (s, 30H, C_5Me_5); ESI-MS (m/z): 904.3 $[\text{M}^{2+} + \text{PF}_6^-]^+$, 485.2 $[\text{M} - \text{PF}_6]^+$; IR (KBr, cm^{-1}): 845s $\nu_{(\text{P-F})}$, 1592m, 1558m, 1522m ($\nu_{\text{C=N}}$ L1), 2995m, 3447w; UV-Vis {acetonitrile, λ_{\max} nm ($\epsilon 10^{-5} \text{M}^{-1} \text{cm}^{-1}$): 271(0.18), 315(0.81), 380(0.11).

2.7.2. $\{[(\text{Cp}^*)\text{RhCl}_2(\text{L2})](\text{PF}_6)_2\}$ (**[20]**(PF_6)₂)

Yield: 60 mg, 70.5%.

Elemental Anal. Calc. for $\text{C}_{32}\text{H}_{42}\text{N}_6\text{Rh}_2\text{Cl}_2\text{P}_2\text{F}_{12}$ (1077.36): C, 35.67; H, 3.93; N, 7.80. Found: C, 35.26; H, 3.99; N, 7.61%. ^1H NMR (400 MHz, CD_3CN): $\delta = 9.05$ (s, 1H), 8.46 (d, 2H, $^3J = 6.0$ Hz), 8.12 (s, 1H), 6.79 (d, 2H, $^3J = 4.6$ Hz), 2.76 (s, 3H, CH_3), 2.73 (s, 3H, CH_3), 1.77 (s, 30H, C_5Me_5); ESI-MS (m/z): 513.8 $[\text{M} - \text{PF}_6]^+$, 932.1 $[\text{M}^{2+} + \text{PF}_6^-]^+$, 513.8 $[\text{M} - \text{PF}_6]^+$; IR (KBr, cm^{-1}): 845s $\nu_{(\text{P-F})}$, 1598m, 1559m, 1521m ($\nu_{\text{C=N}}$ L2), 2998m, 3449w; UV-Vis {acetonitrile, λ_{\max} nm ($\epsilon 10^{-5} \text{M}^{-1} \text{cm}^{-1}$): 259(0.11), 315(0.51), 380(0.08).

2.7.3. $\{[(\text{Cp}^*)\text{RhCl}_2(\text{L3})](\text{PF}_6)_2\}$ (**[21]**(PF_6)₂)

Yield: 67 mg, 77.1%.

Elemental Anal. Calc. for $\text{C}_{34}\text{H}_{46}\text{N}_6\text{Rh}_2\text{Cl}_2\text{P}_2\text{F}_{12}$ (1105.41): C, 36.94; H, 4.19; N, 7.60. Found: C, 36.86; H, 4.15; N, 7.58%. ^1H NMR (400 MHz, CD_3CN): $\delta = 9.09$ (s, 1H), 7.36 (s, 1H), 6.79 (s, 2H), 2.84 (s, 6H, CH_3), 2.79 (s, 6H, CH_3), 1.88 (s, 30H, C_5Me_5); ESI-MS (m/z): 960.2 $[\text{M}^{2+} + \text{PF}_6^-]^+$, 541.81 $[\text{M} - \text{PF}_6]^+$; IR (KBr, cm^{-1}): 843s $\nu_{(\text{P-F})}$, 1601m, 1557m, 1524m ($\nu_{\text{C=N}}$ L3), 3010m, 3442w; UV-Vis {acetonitrile, λ_{\max} nm ($\epsilon 10^{-5} \text{M}^{-1} \text{cm}^{-1}$): 269(0.18), 315(0.48), 371(0.10).

2.7.4. $\{[(\text{Cp}^*)\text{IrCl}_2(\text{L1})](\text{PF}_6)_2\}$ (**[22]**(PF_6)₂)

Yield: 72 mg, 75.7%.

Elemental Anal. Calc. for $\text{C}_{30}\text{H}_{38}\text{N}_6\text{Ir}_2\text{Cl}_2\text{P}_2\text{F}_{12}$ (1227.93): C, 29.34; H, 3.12; N, 6.84. Found: C, 29.23; H, 3.15; N, 6.71%. ^1H NMR (400 MHz, CD_3CN): $\delta = 9.01$ (s, 1H), 8.84 (d, 2H, $^3J = 3.2$ Hz), 8.41 (d, 2H, $^3J = 2.4$ Hz), 8.03 (s, 1H), 6.95 (dd, 2H, $^3J = 1.6$ Hz), 1.79 (s, 30H, C_5Me_5); ESI-MS (m/z): 1082.2 $[\text{M}^{2+} + \text{PF}_6^-]^+$, 575.2 $[\text{M} - \text{PF}_6]^+$; IR (KBr, cm^{-1}): 845s $\nu_{(\text{P-F})}$, 1598m, 1559m, 1521m ($\nu_{\text{C=N}}$ L1), 2995m, 3447w; UV-Vis {acetonitrile, λ_{\max} nm ($\epsilon 10^{-5} \text{M}^{-1} \text{cm}^{-1}$): 260(0.19), 310(0.67), 368(0.11).

2.7.5. $\{[(\text{Cp}^*)\text{IrCl}_2(\text{L2})](\text{PF}_6)_2\}$ (**[23]**(PF_6)₂)

Yield: 60 mg, 61%.

Elemental Anal. Calc. for $\text{C}_{32}\text{H}_{42}\text{N}_6\text{Ir}_2\text{Cl}_2\text{P}_2\text{F}_{12}$ (1255.98): C, 30.60; H, 3.37; N, 6.69. Found: C, 30.45; H, 3.48; N, 6.51%. ^1H NMR (400 MHz, CD_3CN): $\delta = 9.01$ (s, 1H), 8.48 (d, 2H, $^3J = 6.4$ Hz), 8.15 (s, 1H), 6.71 (d, 2H, $^3J = 4.6$ Hz), 2.63 (s, 6H, CH_3), 1.75 (s, 30H, C_5Me_5); ESI-MS (m/z): 1111.1 $[\text{M}^{2+} + \text{PF}_6^-]^+$, 603.1 $[\text{M} - \text{PF}_6]^+$; IR (KBr, cm^{-1}): 844s $\nu_{(\text{P-F})}$, 1599m, 1560m, 1525m ($\nu_{\text{C=N}}$ L2), 3002m, 3441w; UV-Vis {acetonitrile, λ_{\max} nm ($\epsilon 10^{-5} \text{M}^{-1} \text{cm}^{-1}$): 265(0.16), 315(0.56), 371(0.09).

2.7.6. $\{[(\text{Cp}^*)\text{IrCl}_2(\text{L3})](\text{PF}_6)_2\}$ (**[24]**(PF_6)₂)

Yield: 74 mg, 74%.

Elemental Anal. Calc. for $\text{C}_{34}\text{H}_{46}\text{N}_6\text{Ir}_2\text{Cl}_2\text{P}_2\text{F}_{12}$ (1284.04): C, 31.80; H, 3.61; N, 6.54. Found: C, 31.76; H, 3.78; N, 6.33%. ^1H NMR (400 MHz, CD_3CN): $\delta = 9.04$ (s, 1H), 7.31 (s, 1H), 6.68 (s, 2H), 2.83 (s, 6H, CH_3), 2.79 (s, 6H, CH_3), 1.82 (s, 30H, C_5Me_5); ESI-MS (m/z): 1139.5 $[\text{M}^{2+} + \text{PF}_6^-]^+$, 631.2 $[\text{M} - \text{PF}_6]^+$; IR (KBr, cm^{-1}): 843s $\nu_{(\text{P-F})}$, 1608m, 1562m, 1524m ($\nu_{\text{C=N}}$ L3), 3016m, 3450w; UV-Vis {acetonitrile, λ_{\max} nm ($\epsilon 10^{-5} \text{M}^{-1} \text{cm}^{-1}$): 268(0.19), 321(0.61), 376(0.13).

3. Results and discussion

3.1. Syntheses of ligands and complexes

Ligands L2 and L3 were prepared from the corresponding pyrazolato anion and 4,6-dichloropyrimidine. Reaction of half equivalent of dinuclear arene ruthenium complexes $[(\eta^6\text{-arene})\text{Ru}(\mu\text{-Cl})\text{Cl}]_2$ (arene = C_6H_6 , $p\text{-}^i\text{PrC}_6\text{H}_4\text{Me}$) with one equivalent of 4,6-disubstituted pyrimidine ligands *viz.* 4,6-bis(pyrazolyl)pyrimidine (L1), 4,6-bis(3-methyl-pyrazolyl)pyrimidine (L2) or 4,6-bis(3,5-dimethyl-pyrazolyl)pyrimidine (L3) in methanol generates the mononuclear complexes $[(\eta^6\text{-C}_6\text{H}_6)\text{Ru}(\text{L})\text{Cl}]^+$ (L = L1, **1**; L2, **2**; L3, **3**), $[(\eta^6\text{-}p\text{-}^i\text{PrC}_6\text{H}_4\text{Me})\text{Ru}(\text{L})\text{Cl}]^+$ (L = L1, **4**; L2, **5**; L3, **6**), respectively (Scheme 2). The homologous complexes with two coordinated arene ruthenium fragments, $\{[(\eta^6\text{-C}_6\text{H}_6)\text{RuCl}]_2(\text{L})\}(\text{PF}_6)_2$ (L = L1, **13**; L2, **14**; L3, **15**) and $\{[(\eta^6\text{-}p\text{-}^i\text{PrC}_6\text{H}_4\text{Me})\text{RuCl}]_2(\text{L})\}(\text{PF}_6)_2$ (L = L1, **16**; L2, **17**; L3, **18**), were prepared when a 1:1 M ratio was used and over prolonged reaction times (Scheme 2). All these cationic ruthenium complexes were isolated as their hexafluorophosphate salts.

Similarly, the reaction of half equivalent of the dimeric chloro-bridged complexes $[(\text{Cp}^*)\text{M}(\mu\text{-Cl})\text{Cl}]_2$ (M = Rh, Ir) with 4,6-disubstituted-pyrimidine ligands (L) in methanol generates the mononuclear

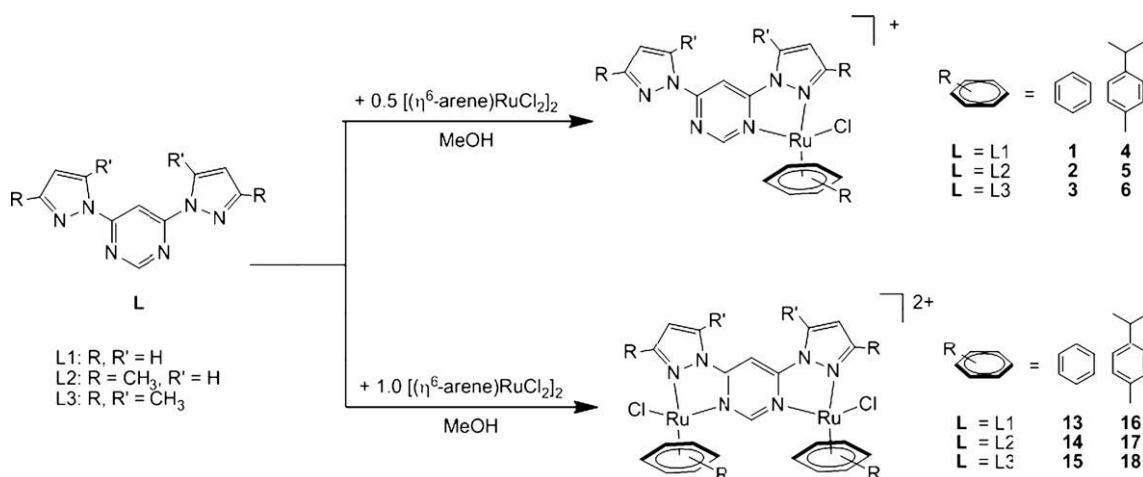
cationic complexes of the type $[(\text{Cp}^*)\text{Rh}(\text{L})\text{Cl}]^+$ (L = L1, **7**; L2, **8**; L3, **9**), $[(\text{Cp}^*)\text{Ir}(\text{L})\text{Cl}]^+$ (L = L1, **10**; L2, **11**; L3, **12**), respectively (Scheme 3). The homologous complexes with two coordinated Cp^*Rh or Cp^*Ir fragments, $\{[(\text{Cp}^*)\text{RhCl}]_2(\text{L})\}(\text{PF}_6)_2$ (L = L1, **19**; L2, **20**; L3, **21**) and $\{[(\text{Cp}^*)\text{IrCl}]_2(\text{L})\}(\text{PF}_6)_2$ (L = L1, **22**; L2, **23**; L3, **24**), were prepared when a 1:1 M ratio was used and at prolonged reaction times (Scheme 3). All these cationic rhodium or iridium complexes were isolated as their hexafluorophosphate salts.

When the mononuclear complexes **[1]PF₆** – **[12]PF₆** were further reacted with half mole of arene ruthenium or Cp^*Rh or Ir dimers in acetonitrile solution, no reaction took place and isolated as starting compounds. Also attempts to synthesize hetero-nuclear complexes by reaction of the mononuclear complexes with other metal atoms led to no reaction.

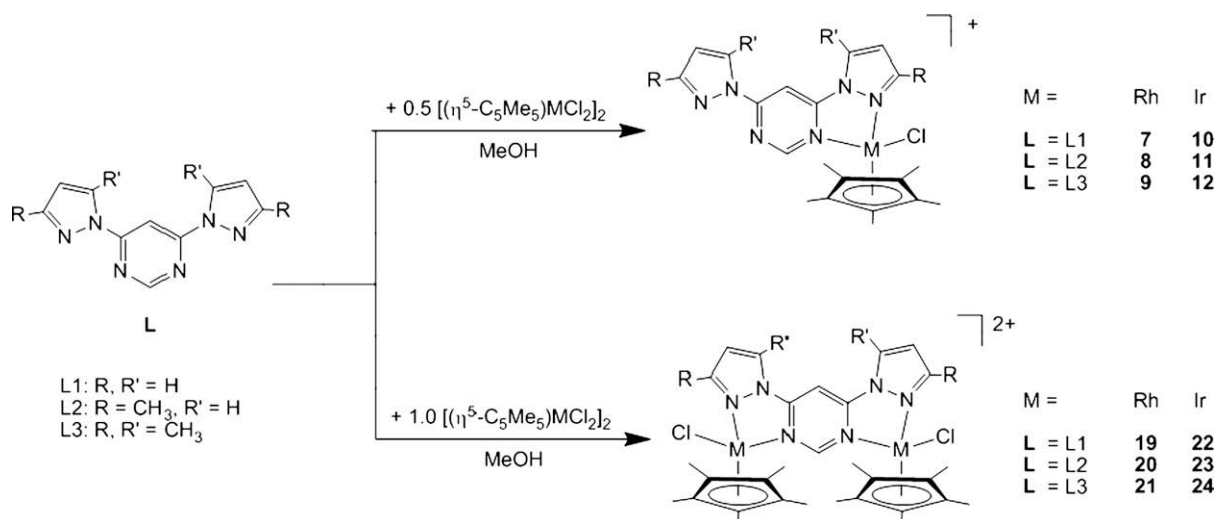
All these complexes are orange yellow in color, non-hygroscopic, air stable solids. They are soluble in acetonitrile but partially soluble in dichloromethane, chloroform and acetone.

3.2. Characterization of mononuclear complexes **1** – **12**

All these mononuclear complexes were characterized by IR, ^1H NMR, mass and elemental analysis. The infrared spectra of the complexes **[1]PF₆** – **[12]PF₆** exhibit a strong band in the region



Scheme 2.



Scheme 3.

844–850 cm^{-1} , a typical $\nu_{\text{P-F}}$ stretching band for the PF_6 anions. Moreover, all complexes show absorption bands around 1600–1610 cm^{-1} , 1550–1558 cm^{-1} and 1522–1528 cm^{-1} corresponding to $\nu_{\text{C=N}}$ vibrations of pyrazole and pyrimidine moieties [52] besides these absorptions 2990–3050 and 3400–3450 were observed.

The mass spectra of these complexes exhibited, as expected, the corresponding molecular ion peaks m/z at 427, 455, 483, 483, 511, 538, 485, 513, 541, 575, 603 and 631. For instance complex **[1]** PF_6 shown four fragments, a molecular ion peak at 427 $[\text{M}]^+$, 391 $[\text{M}-\text{Cl}]^+$, 313 $[\text{M}-\text{Cl-arene}]^+$ and 213 $[\text{L}+1]$.

The ^1H NMR spectra of the free ligands L1–L3 exhibit a characteristic set of five resonances for the eight protons of pyrazole and pyrimidine rings, since the pyrazole rings are in symmetrical position. Upon coordination with the metal atom, each mononuclear complex has shown seven to eight set of resonances for the ligand L1–L3 protons in the region $\delta = 9.56$ – 6.78 , $\delta = 9.41$ – 2.43 , and $\delta = 9.34$ – 2.17 , respectively. It indicates the formation of mononuclear complexes. The resonances of the coordinated pyrazole and pyrimidine rings protons shifted to higher frequency as a consequence of their coordination to the ruthenium or rhodium or iridium atom. However, arene ruthenium complexes **[1]** PF_6 – **[6]** PF_6 , the resonances of ligand protons significantly shifted to down field compared to Cp^*Rh or Cp^*Ir complexes, **[7]** PF_6 – **[12]** PF_6 . Besides these ligand resonances, complexes **[1]** PF_6 – **[3]** PF_6 exhibit a singlet for the benzene ring protons at $\delta = 6.20$ – 5.93 , complexes **[4]** PF_6 to **[6]** PF_6 exhibit a septet at $\delta = 2.70$ for the protons of the isopropyl group and a singlet at $\delta = 2.17$ for the methyl protons of the *p*-cymene ring. The ring protons and methyl protons of the isopropyl group of the *p*-cymene ligand have shown an unusual pattern of resonances. For instance, the methyl protons of the isopropyl group displays two doublets at *ca.* $\delta = 1.18$ – 1.07 , instead of one doublet as in the starting complex. The aromatic protons of the *p*-cymene ligand display four doublets, instead of two doublets as in the starting precursor. This unusual pattern is due to the diastereotopic methyl protons of the isopropyl group and aromatic protons of the *p*-cymene ligand since the ruthenium atom is stereogenic due to the coordination of four different ligand atoms [53,54]. Complexes **[1]** PF_6 to **[12]** PF_6 exhibit a singlet at $\delta = 1.71$ – 1.55 for the five methyl groups of the Cp^* ligand. The chemical shift of the co-ligands arene or Cp^* ring protons are shifted to down field compared to the starting precursors.

3.3. Molecular structure of selected mononuclear complexes

The molecular structure of the $[(\eta^6\text{-C}_6\text{H}_6)\text{Ru}(\text{L3})\text{Cl}]\text{PF}_6$ (**[3]** PF_6), $[(\eta^6\text{-}p\text{-}^i\text{PrC}_6\text{H}_4\text{Me})\text{Ru}(\text{L3})\text{Cl}]\text{PF}_6$ (**[6]** PF_6) as well as the Cp^* rhodium complex $[(\text{Cp}^*)\text{Rh}(\text{L1})\text{Cl}]\text{PF}_6$ (**[7]** PF_6) have been established by single crystal X-ray structure analysis. These cationic complexes show a typical piano-stool geometry with the metal center being coordinated by an aromatic ligand, a terminal chloro ligand and a chelating 4,6-disubstituted-pyrimidine ligand. The metal atom possesses an octahedral arrangement with two *cis*-nitrogen atoms of the pyrazolyl-pyrimidine ligand acting as a bidentate chelating ligand in a five-membered ring chelating fashion involving one nitrogen atom of the pyrazolyl moiety and the nitrogen atom of the pyrimidine group. The structures are shown in Figs. 1–3. Selected bond lengths and angles for **[3]** PF_6 , **[6]** PF_6 and **[7]** PF_6 are presented in Table 2.

In the mononuclear complexes **[3]** PF_6 and **[7]** PF_6 the N1–metal distance (2.076 and 2.106 Å) of the pyrazolyl moiety is slightly shorter than the corresponding pyrimidinyl, N3–metal distance (2.092, and 2.138 Å), in contrast to complex **[6]** PF_6 in which the N1–metal (2.102 Å) distance is slightly longer than the corresponding N3–metal distance (2.093(2) Å). The Rh–N bond distance (2.106(3) and 2.138(3) Å) in **7** is slightly longer than the corresponding distances of ruthenium complex **3** (2.076(3) and 2.092(2) Å) and complex **6** (2.102 and 2.093), while the M–Cl

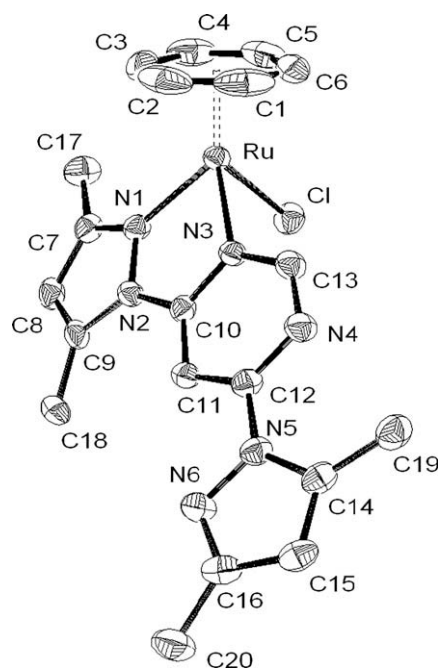


Fig. 1. Molecular structure of **[3]** $\text{PF}_6\cdot\text{H}_2\text{O}$ at 50% probability level. Hydrogen atoms, water molecule and hexafluorophosphate anion have been omitted for clarity.

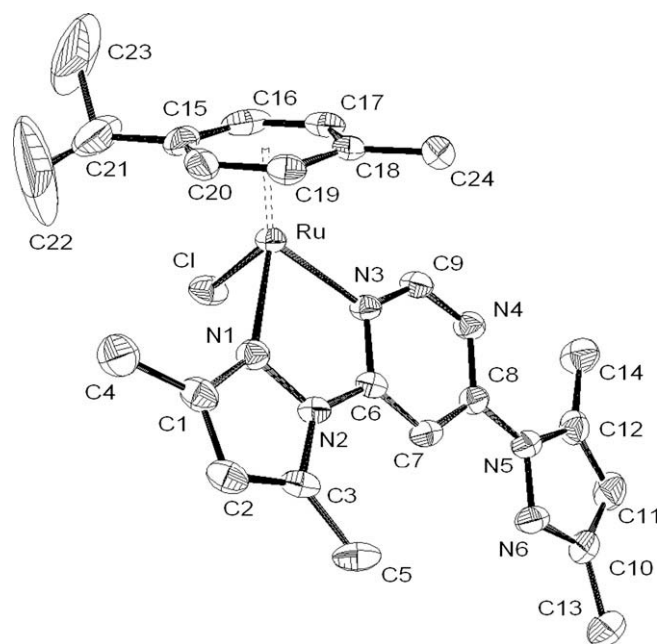


Fig. 2. Molecular structure of **[6]** PF_6 at 50% probability level. Hydrogen atoms and hexafluorophosphate anion have been omitted for clarity.

[2.402(7), 2.388(8) and 2.400(6)] bond lengths show no significant differences in all the cations and similar reported values [55,56]. The N–M–N bond angles [75.33(7) in **3** and 75.56°(9) in **6**] are similar to that of complexes $[(\eta^6\text{-}p\text{-}^i\text{PrC}_6\text{H}_4\text{Me})\text{RuCl}(2,3\text{-bis}(\alpha\text{-pyridyl})\text{quinoxaline})]^+$ [76.2 (2)°] [57]. The distances between the ruthenium atom and the centroid of the C_6 aromatic ring in **3** and **6** are comparable (1.69 and 1.68 Å) but quite shorter than the distance between the rhodium atom and the C_5 aromatic ring observed in **7** (1.77 Å). The M–N1 bond distances [2.076(9) to 2.102(2) Å] are comparable to those in $\text{g}_6\text{-}p\text{-}^i\text{PrC}_6\text{H}_4\text{Me}$

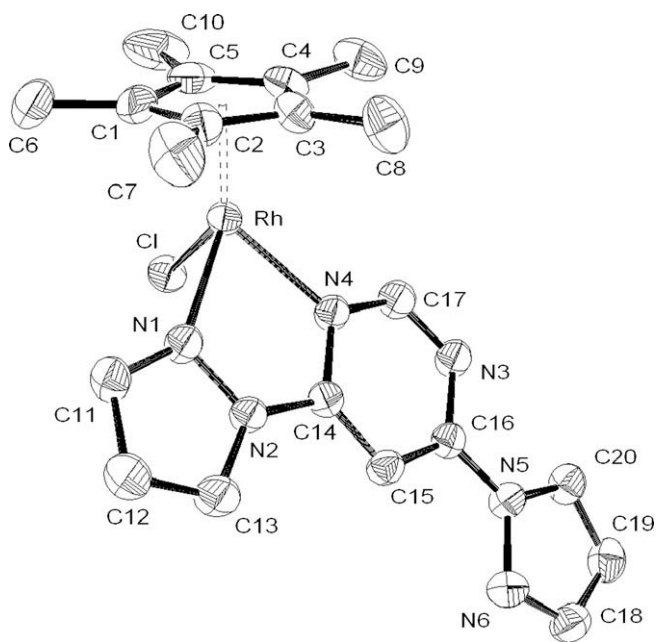


Fig. 3. Molecular structure of $[7]PF_6$ at 50% probability level. Hydrogen atoms and anion have been omitted for clarity.

$[(\eta^6-C_6H_6)RuCl(2-(1\text{-imidazol-2-yl})pyridine)]^+$ [58] and $[(Cp^*)Ir(2-(2'\text{-pyridyl})\text{-imidazole})Cl]^+$ [59].

As amplified in Figs. 1–3, all cations possess metal-centered chirality as the metal atom is coordinated to four different ligator atoms. However, since none of the ligands contain chiral centers, they are all obtained as a racemic mixture and they all crystallize in the centrosymmetric space group $P\bar{1}$.

In the crystal packing of $[3]PF_6 \cdot H_2O$, the hexafluorophosphate anion sits on side of the cationic complex and interacts with an

hydrogen atom of the C_6H_6 ligand (see supplementary material). The hexafluorophosphate anion interacts with C_6H_6 ligand through C–H···F contacts: the C···F distances being 3.22 and 3.26 Å with C–H···F angles of 148.9 and 138.3°, respectively. In addition to this the oxygen atom interacts with one of the hydrogen atoms of ligand L1 through C–H···O contact: the C···O distance being 3.10 Å and C–H···O angle is 149.06°.

3.4. Characterization of the dinuclear complexes

The infrared spectra of the dinuclear complexes $[13](PF_6)_2$ – $[24](PF_6)_2$ exhibit a similar trend as for the mononuclear complexes $[1]PF_6$ – $[12]PF_6$. The mass spectra of these complexes exhibited two main peaks; a minor peak with an approximately 50% intensity attributed to $[M-PF_6]^+$ at m/z 786, 814, 842, 898, 926, 954, 904, 932, 960, 1082, 1110 and 1138, respectively, and a major peak which corresponds to the loss of an $[(\text{arene}/Cp^*)MCl]^+$ fragment, thus giving the corresponding mononuclear cations $[1-PF_6]^+$ – $[12-PF_6]^+$ at m/z = 427, 455, 483, 483, 511, 538, 485, 513, 541, 575, 603 and 631.

The 1H NMR spectra of the dinuclear complexes $[13](PF_6)_2$ – $[24](PF_6)_2$, exhibit five distinct resonances, which are assigned to pyrazole or substituted pyrazoles and pyrimidine ring protons of the ligand L1 or L2 or L3, indicating the formation of dinuclear complexes. The number of distinct resonances of these complexes is similar to the number of distinct resonances of free ligands, indicating that the pyrazole rings of the ligands remain symmetrical even after formation of the complexes. These results indicate the formation of dinuclear complexes. The resonances of the coordinated pyrazole and pyrimidine protons shifted to considerable down field as compared to mononuclear complexes, a consequence of their coordination to two ruthenium, rhodium or iridium atoms. However, in the arene ruthenium complexes $[13](PF_6)_2$ – $[18](PF_6)_2$, the resonances of the ligand protons significantly shifted to down field compared to Cp^*Rh or Ir complexes, $[19](PF_6)_2$ – $[24](PF_6)_2$. Besides these resonances complexes

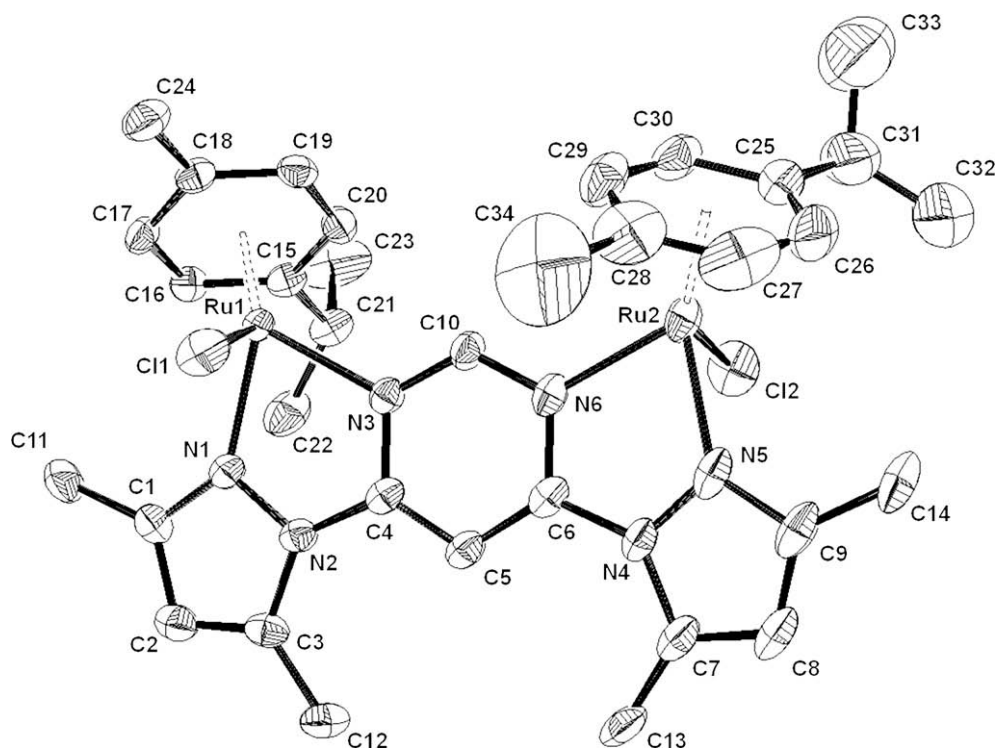


Fig. 4. Molecular structure of $[18](PF_6)_2 \cdot H_2O$ at 50% probability level. Hydrogen atoms, water molecule and hexafluorophosphate anions have been omitted for clarity.

[13](PF₆)₂ – [15](PF₆)₂ exhibit a singlet for both benzene ring protons at $\delta = 6.24$ and 6.15 ppm, complexes [16](PF₆)₂ – [18](PF₆)₂ exhibit a similar trend like the mononuclear complexes [4]PF₆ – [4]PF₆. A septet at $\delta = 2.70$ for the protons of the isopropyl group, a singlet at $\delta = 2.17$ for the methyl protons of *p*-cymene ring, four doublets *ca.* $\delta = 6.09$ –5.93 for the ring protons of the *p*-cymene ligand and finally methyl protons of the isopropyl group displays two doublets at *ca.* $\delta = 1.18$ and 1.07. Complexes [19](PF₆)₂ – [24](PF₆)₂ exhibit a singlet in the region $\delta = 1.88$ –1.77 for the five methyl groups of the Cp* ligand. The chemical shift of the arene co-ligands or Cp* ring protons are shifted to higher frequency compared to the starting precursors as well as compared to the mononuclear complexes.

3.5. Molecular structure of the dinuclear complex [18](PF₆)₂

The molecular structure of $\{[(\eta^6\text{-}p\text{-Pr}^i\text{C}_6\text{H}_4\text{Me})\text{RuCl}]_2(\text{L3})\}^{2+}$ ([18](PF₆)₂) has been established by single crystal X-ray structure analysis. Selected bond lengths and angles are presented in Table 2. The dinuclear complex [18](PF₆)₂ shows a typical piano-stool geometry for the ruthenium atoms with the metal centers being coordinated by the aromatic ligand, a terminal chloride and a chelating *N,N*-ligand (Fig. 4). The compound [18](PF₆)₂ contains two Ru(II) metal centers which are bonded to a $\eta^6\text{-}p\text{-Pr}^i\text{C}_6\text{H}_4\text{Me}$ ligand and bridged by the L3 ligand through its nitrogen atoms. Interestingly, the dinuclear complex [18](PF₆)₂ reveals a *trans* conformation of the two chloro ligands (Fig. 4). The distance between the ruthenium atoms and the corresponding centroid of the $\eta^6\text{-}p\text{-Pr}^i\text{C}_6\text{H}_4\text{Me}$ ring is 1.68 and 1.67 Å. These distances are comparable to those in the related complex cation $[(\eta^6\text{-}p\text{-Pr}^i\text{C}_6\text{H}_4\text{Me})\text{Ru}(2\text{-acetylthiazoleazine})\text{Cl}]^+$ [60].

The Ru–N bond distances ranging from 2.072(3) to 2.092(3) Å are shorter than in the mononuclear complex [6]PF₆ [2.102(3) and 2.093(3) Å], interestingly the Ru to N1 or N5 (pyrazole) distances are shorter than the Ru–N3 or N6 (pyrimidine) distances in the dinuclear complex [18](PF₆)₂, where as it is opposite in mononuclear complex [6]PF₆, while the ruthenium–chlorine bond

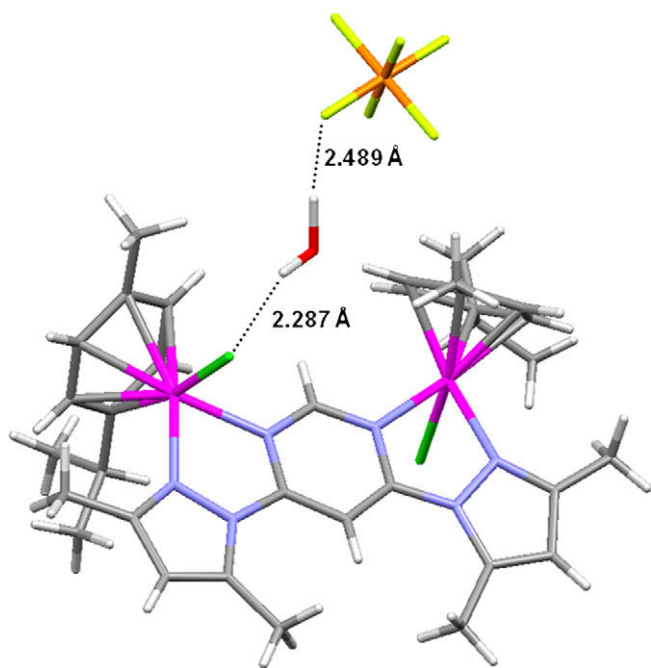


Fig. 5. Hydrogen bond network in [18](PF₆)₂·H₂O showing the intermolecular interactions involving an hexafluorophosphate anion, a water molecule and cation [18]⁺.

distances are comparable. In complex [18](PF₆)₂, the isopropyl group of the *p*-cymene ligand at Ru1 center located opposite to the halide ligand in order to reduce steric interactions, while at Ru2 the isopropyl group is located on same side to the halide ligand.

Complex [18](PF₆)₂ crystallizes with one molecule of water per asymmetric unit, forming an hydrogen-bonded network to the chloride atom and the fluorine atom of the hexafluorophosphate anion (Fig. 5). The water molecule interacts with chloride ligand through O–H···Cl contacts: the O···Cl distance being 3.26 Å with an O–H···Cl angle of 156.3°. In addition to this, the water molecule interacts with one of the fluoride atoms of the hexafluorophosphate anion through F···H–O contacts: the F···O distance being 3.51 Å and the F···H–O angle 154.09°.

4. UV-Vis spectroscopy

Electronic absorption spectra of the mononuclear complexes [1]PF₆ – [12]PF₆ as well as the dinuclear complexes [13](PF₆)₂ – [24](PF₆)₂ were acquired in acetonitrile, at 10^{–5} M concentration in the range 250–550 nm. Electronic spectra of representative complexes are depicted in Fig. 6. The spectra of these complexes are characterized by two main features, *viz.*, an intense ligand-localized or intra-ligand $\pi \rightarrow \pi^*$ transition in the ultraviolet region and metal-to-ligand charge transfer (MLCT) $d\pi(\text{M}) \rightarrow \pi^*(\text{L1} - \text{ligand})$ bands in the visible region [61]. Since the low spin d^6 configuration of the mononuclear complexes provides filled orbitals of suitable symmetry at the Ru(II), Rh(III) and Ir(III) centers, these can interact with low lying π^* orbitals of the ligands. All these mononuclear complexes [1]PF₆ – [12]PF₆ show two medium intensity bands in the region 261–310 nm, an intense band in the region 340–380 nm in UV region and a low energy absorption band in the visible region 450–470 nm. Where as the dinuclear complexes [13](PF₆)₂ – [24](PF₆)₂ shown similar number of bands in higher frequency region, for instance a medium intensity band in the region 260–275 nm, a high intensity band in the region 318–322 nm and a broad band in the region 356–418 nm. The medium intensity bands in UV region is assigned to $\pi\text{-}\pi^*$, a high intensity band in UV region is assigned to inter and intra-ligand $\pi\text{-}\pi^*/n\text{-}\pi^*$ transitions [62,63], while the low energy absorption band in the visible region is assigned to metal-to-ligand charge transfer (MLCT) ($t_{2g}\text{-}\pi^*$).

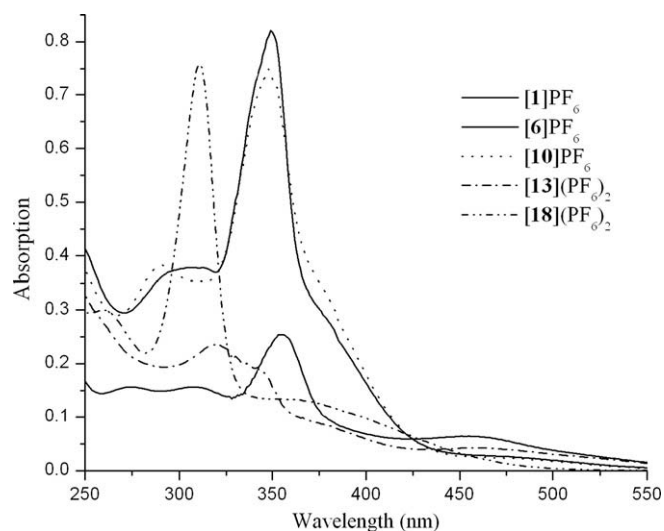


Fig. 6. UV-Vis electronic spectra of selected complexes in acetonitrile at 298 K.

5. Conclusions

We have described and characterized new mono and dinuclear ruthenium, rhodium and iridium complexes with the ligands L1, L2 and L3, in good yield, which are remarkably stable in air as well as in solution. In both, mono and dinuclear complexes, the metal atom are bonded with the N-atom of the pyrazole moiety and the N-atom of the pyrimidine moiety. But our effort to make hetero-nuclear complexes by using second binding site of the mono-nuclear complexes was unsuccessful, since coordination of the first metallic center does not induce the bonding in the second position in a kind of chemical symbiosis driven by the ligand or the metal center.

Acknowledgement

K. Mohan Rao gratefully acknowledges the Department of Science and Technology, New Delhi, (Sanction Order No. SR/S1/IC-11/2004) for the financial support.

Appendix A. Supplementary material

CCDC 742491, 742492, 742493 and 751116 contain the supplementary crystallographic data for **3**, **6**, **7** and **18**. These data can be obtained free of charge from The Cambridge Crystallographic Data Center via www.ccdc.cam.ac.uk/data_request/cif. Supplementary data associated with this article can be found, in the online version, at doi:10.1016/j.jorgchem.2009.11.030.

References

- [1] S. Trofimenko, *Chem. Rev.* 93 (1993) 943.
- [2] M.D. Ward, *Rep. Prog. Chem., Sect. A: Inorg. Chem.* 91 (1994) 317.
- [3] A. Juris, S. Barigelletti, S. Campagna, V. Balzani, P. Belsler, A. von Zelewsky, *Coord. Chem. Rev.* (1988) 27.
- [4] J.A. Bailey, M.G. Hill, R.E. Marsh, V.M. Miskowski, W.P. Schaefer, H.B. Gray, *Inorg. Chem.* 34 (1995) 4591.
- [5] M.G. Hill, J.A. Bailey, V.M. Miskowski, H.B. Gray, *Inorg. Chem.* 35 (1996) 4585.
- [6] P.-I. Kvam, M.V. Puzyk, V.S. Cotlyr, J. Songstad, K.P. Balashev, *Acta Chem. Scand.* 50 (1996) 6.
- [7] E.W. Abel, A. Gelling, K.G. Orrell, A.G. Osborne, V. Sjöik, *Chem. Commun.* (1996) 2329.
- [8] E.W. Abel, K.G. Orrell, A.G. Osborne, H.M. Pain, V. Sjöik, M.B. Hursthouse, K.M.A. Malik, *Chem. Commun.* (1996) 253.
- [9] M. Akiba, Y. Sasaki, *Inorg. Chem. Commun.* 1 (1998) 61.
- [10] A. Gelling, K.G. Orrell, A.G. Osborne, V. Sjöik, *J. Chem. Soc., Dalton Trans.* (1998) 937.
- [11] M. Navarro, W.F.D. Giovanni, J.R. Romero, *Synth. Commun.* 20 (1990) 399.
- [12] N. Grover, H.H. Thorp, *J. Am. Chem. Soc.* 113 (1991) 7030.
- [13] X. Hua, M. Shang, A.G. Lappin, *Inorg. Chem.* 36 (1997) 3735.
- [14] C.M. Che, C. Ho, T.C. Lau, *J. Chem. Soc., Dalton Trans.* (1991) 901.
- [15] S.J. Raven, T.J. Meyer, *Inorg. Chem.* 27 (1988) 4478.
- [16] C.M. Che, W.T. Tang, W.O. Lee, K.Y. Wong, T.C. Lau, *J. Chem. Soc., Dalton Trans.* (1992) 1551.
- [17] A. Dvletoglou, S.A. Adeyemi, M.N. Lynn, D.J. Hodgson, T.J. Meyer, *J. Am. Chem. Soc.* 112 (1990) 8989.
- [18] C.M. Che, V.W.W. Yam, *Adv. Inorg. Chem.* 39 (1992) 233.
- [19] R.A. Binstead, M.E. Mc Guire, A. Dvletoglou, W.K. Seok, L.E. Roecker, T.J. Meyer, *J. Am. Chem. Soc.* 114 (1992) 173.
- [20] A.W. Stumpf, E. Saive, A. Demonceau, A.F. Noels, *J. Chem. Soc., Chem. Commun.* (1995) 1127.
- [21] O. Zava, S.M. Zakeeruddin, C. Danelon, H. Vogel, M. Grätzel, P.J. Dyson, *ChemBioChem* 10 (2009) 1796.
- [22] P.C.A. Bruijninx, P.J. Sadler, *Adv. Inorg. Chem.* 61 (2009) 1.
- [23] F. Schmitt, P. Govindaswamy, O. Zava, G. Süss-Fink, L. Juillerat-Jeanneret, B. Therrien, *J. Biol. Inorg. Chem.* 14 (2009) 101.
- [24] B. Therrien, G. Süss-Fink, P. Govindaswamy, A.K. Renfrew, P.J. Dyson, *Angew. Chem., Int. Ed.* 47 (2008) 3773.
- [25] P. Govender, N.C. Antonels, J. Mattsson, A.K. Renfrew, P.J. Dyson, J.R. Moss, B. Therrien, G.S. Smith, *J. Organomet. Chem.* 694 (2009) 3470.
- [26] N.P.E. Barry, N.H. Abd Karim, R. Vilar, B. Therrien, *Dalton Trans.* (2009), doi:10.1039/b913642h.
- [27] L. Rigamonti, F. Demartin, A. Forni, S. Righetto, A. Pasini, *Inorg. Chem.* 45 (2006) 10976.
- [28] J. Gradinaru, A. Forni, V. Druta, F. Tessore, S. Zecchin, S. Quici, N. Garbalau, *Inorg. Chem.* 46 (2007) 884.
- [29] G. Gupta, K.T. Prasad, B. Das, G.L.P. Yap, K. Mohan Rao, *J. Organomet. Chem.* 694 (2009) 2618.
- [30] L. Soriano, F.A. Jalón, B.R. Manzano, M. Maestro, *Inorg. Chim. Acta* 362 (2009) 4486.
- [31] K. Sarjit Singh, Y.A. Mozharivskiy, K. Mohan Rao, *Z. Anorg. Allg. Chem.* 632 (2005) 172.
- [32] K. Sarjit Singh, Y.A. Mozharivskiy, C. Thöne, K. Mohan Rao, *J. Organomet. Chem.* 690 (2005) 3720.
- [33] G. Gupta, G.P.A. Yap, B. Therrien, K. Mohan Rao, *Polyhedron* 28 (2009) 844.
- [34] P. Govindaswamy, Y.A. Mozharivskiy, K. Mohan Rao, *J. Organomet. Chem.* 689 (2004) 3265.
- [35] P. Govindaswamy, P.J. Carroll, Y.A. Mozharivskiy, K. Mohan Rao, *J. Organomet. Chem.* 690 (2005) 885.
- [36] P. Govindaswamy, Y.A. Mozharivskiy, K. Mohan Rao, *Polyhedron* 23 (2004) 3115.
- [37] J.K. Hurst, *Coord. Chem. Rev.* 249 (2005) 313.
- [38] C. Sens, I. Romero, M. Rodriguez, A. Llobet, T. Parella, J.B. Buchholz, *J. Am. Chem. Soc.* 126 (2004) 7798.
- [39] I. Romero, M. Rodriguez, C. Sens, J. Mola, *Inorg. Chem.* 47 (2008) 1824–1834.
- [40] M.A. Bennett, T.N. Huang, T.W. Matheson, A.K. Smith, *Inorg. Synth.* 21 (1982) 74.
- [41] M.A. Bennett, T.W. Matheson, G.B. Robertson, A.K. Smith, P.A. Tucker, *Inorg. Chem.* 19 (1980) 1014.
- [42] M.A. Bennett, A.K. Smith, *J. Chem. Soc., Dalton Trans.* (1974) 233.
- [43] J.W. Kang, K. Moseley, P.M. Maitlis, *J. Am. Chem. Soc.* 91 (1969) 5970.
- [44] R.G. Ball, W.A.G. Graham, D.M. Heinekey, J.K. Hoyano, A.D. McMaster, B.M. Mattson, S.T. Michel, *Inorg. Chem.* 29 (1990) 2023.
- [45] C. White, A. Yates, P.M. Maitlis, *Inorg. Synth.* 29 (1992) 228.
- [46] M. Ikeda, K. Maruyama, Y. Nobuhara, T. Yamada, S. Okabe, *Chem. Pharm. Bull.* 45 (1997) 549.
- [47] R. Uson, L.A. Oro, M. Esteban, *Polyhedron* 3 (1984) 213.
- [48] G.M. Sheldrick, *Acta Crystallogr., Sect. A46* (1990) 467.
- [49] G.M. Sheldrick, *SHELXL-97*, University of Göttingen, Göttingen, Germany, 1999.
- [50] L.J. Farrugia, *J. Appl. Crystallogr.* 30 (1997) 565.
- [51] I.J. Bruno, J.C. Cole, P.R. Edgington, M. Kessler, C.F. Macrae, P. McCabe, J. Pearson, R. Taylor, *Acta Crystallogr., Sect. B58* (2002) 389.
- [52] H. van der Poel, G. van Koten, K. Vrieze, *Inorg. Chem.* 19 (1980) 1145.
- [53] P. Govindaswamy, B. Therrien, G. Süss-Fink, P. Štěpnička, Ludvík, *J. Organomet. Chem.* 692 (2007) 1661.
- [54] K.T. Prasad, B. Therrien, K.M. Rao, *J. Organomet. Chem.* 693 (2008) 3049.
- [55] K.T. Prasad, B. Therrien, K.M. Rao, *J. Organomet. Chem.* (2009), doi:10.1016/j.jorgchem.2009.10.007.
- [56] B. Therrien, C. Sa-Mohamed, G. Süss-Fink, *Inorg. Chim. Acta* 361 (2008) 2601.
- [57] R. Lalrempuia, K. Mohan Rao, *Polyhedron* 22 (2003) 3155.
- [58] H. Mishra, R. Mukherjee, *J. Organomet. Chem.* 691 (2006) 3545.
- [59] K. Pachhunga, B. Therrien, K.A. Kreisel, G.P.A. Yap, M.R. Kollipara, *Polyhedron* 26 (2007) 3638.
- [60] K.T. Prasad, G. Gupta, A.V. Rao, B. Das, K.M. Rao, *Polyhedron* 28 (2009) 2649.
- [61] E. Binamira-Soriaga, N.L. Keder, W.C. Kaska, *Inorg. Chem.* 29 (1990) 3167.
- [62] C.S. Araújo, M.G.B. Drew, V. Félix, L. Jack, J. Madureira, M. Newell, S. Roche, T.M. Santos, J.A. Thomas, L. Yellowlees, *Inorg. Chem.* 41 (2002) 2250.
- [63] H. Deng, J. Li, K.C. Zheng, Y. Yang, H. Chao, L.N. Ji, *Inorg. Chim. Acta* 358 (2005) 3430.